

## Accepted Manuscript

Structural characterization of wheat starch granules differing in amylose content and functional characteristics

Jaroslav Blazek, Hayfa Salman, Amparo Lopez Rubio, Elliot Gilbert, Tracey Hanley, Les Copeland

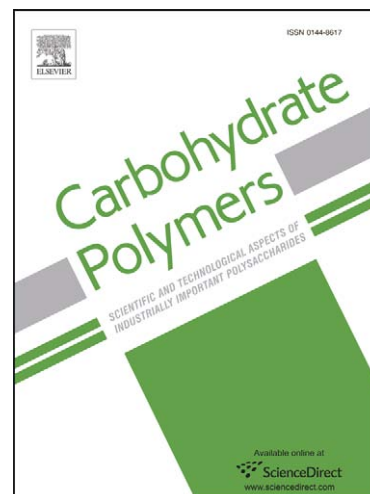
PII: S0144-8617(08)00434-7  
DOI: [10.1016/j.carbpol.2008.09.017](https://doi.org/10.1016/j.carbpol.2008.09.017)  
Reference: CARP 3929

To appear in: *Carbohydrate Polymers*

Received Date: 4 February 2008  
Revised Date: 27 August 2008  
Accepted Date: 12 September 2008

Please cite this article as: Blazek, J., Salman, H., Rubio, A.L., Gilbert, E., Hanley, T., Copeland, L., Structural characterization of wheat starch granules differing in amylose content and functional characteristics, *Carbohydrate Polymers* (2008), doi: [10.1016/j.carbpol.2008.09.017](https://doi.org/10.1016/j.carbpol.2008.09.017)

This is a PDF file of an unedited manuscript that has been accepted for publication. As a service to our customers we are providing this early version of the manuscript. The manuscript will undergo copyediting, typesetting, and review of the resulting proof before it is published in its final form. Please note that during the production process errors may be discovered which could affect the content, and all legal disclaimers that apply to the journal pertain.





26 starch as a distinctive comparison with the other samples confirmed a general trend of  
27 increasing amylose content being linked with the accumulation of defects within crystalline  
28 lamellae. We conclude that amylose content directly influences the architecture of  
29 semicrystalline lamellae, whereas thermodynamic and functional properties are brought about  
30 by the interplay of amylose content and amylopectin architecture.

31

32 **Keywords:** Wheat starch, *Triticum aestivum*, amylose, amylopectin, small-angle X-ray  
33 scattering, granule structure, X-ray diffraction, differential scanning calorimetry.

34

## 35 INTRODUCTION

36

37 Semicrystalline native starch granules display a hierarchical structural periodicity. Starch  
38 granules have a layered organization with alternating amorphous and semicrystalline radial  
39 growth rings of 120 to 400 nm thickness emanating from the hilum. The amorphous rings  
40 consist of amylose and amylopectin in a disordered conformation, whereas the semicrystalline  
41 rings are formed by a lamellar structure of alternating crystalline and amorphous regions with  
42 a repeat distance of 9 to 11 nm (Cameron & Donald, 1992). The crystalline regions of the  
43 lamellae are mainly formed by double helices of amylopectin side chains packed laterally into  
44 a crystalline lattice, whereas amorphous regions contain amylose and the amylopectin  
45 branching points. Amylopectin clusters may contain amylose molecules that pass through  
46 both the crystalline and amorphous layers. These “tie-chain” amylose molecules are proposed  
47 to be in a straightened conformation in crystalline regions and in a disordered conformation in  
48 amorphous regions (Kozlov et al., 2007a; Matveev et al., 1998).

49

50 Small-angle X-ray scattering (SAXS) techniques measure differences in electron density  
51 distribution, whereas diffraction techniques are indicative of crystallinity of the material.  
52 SAXS and neutron scattering have been shown to be useful for studying the arrangement of  
53 lamellar structures in semi-crystalline starch granules (Waigh et al., 1996). SAXS patterns  
54 from hydrated native starches show a broad scattering peak, from which the average thickness  
55 of the lamellar repeat unit (that is the thickness of the crystalline plus amorphous layers) can  
56 be calculated. In combination with other techniques, such as differential scanning calorimetry  
57 (DSC) and X-ray diffraction (XRD), the thickness of the crystalline layer can be calculated  
58 (Blanshard et al., 1984; Waigh et al., 1998, 2000a, 2000b). The position of the SAXS peak is  
59 related to the average lamellar repeat length in granular starches, whereas peak width and  
60 intensity are mainly dependent on the regularity of the arrangement of lamellae and the  
61 electron density differences between the amorphous and crystalline regions of the lamellar  
62 structure. Recent studies using SAXS and high-sensitivity DSC have increased our  
63 understanding of the influence of amylose located within amylopectin clusters in native starch  
64 granules (Kozlov et al., 2006). SAXS has also proved useful in helping to describe processes  
65 such as swelling, gelatinization, retrogradation and annealing (Donald et al., 2001; Lopez-  
66 Rubio et al., 2007; Vermeulen et al., 2005, 2006).

67

68 Several approaches aimed at obtaining wheat starches with increased amylose content have  
69 been reported in the literature. Some of the breeding programs are based on the genetic  
70 manipulation of the enzymes involved in starch synthesis (Kozlov et al., 2006; Morell &  
71 Myers, 2005), whereas selecting among wheat varieties with increased amylose content for  
72 functional characteristics has also been reported to lead towards the increase in amylose  
73 content (Blazek & Copeland, 2008). Different breeding approaches can result in starches with  
74 increased amylose that vary in their functional, structural and thermodynamic characteristics.

75 For example, wheat varieties with increased amylose content described by Hung et al. (2007)  
76 had levels of crystallinity comparable to starches with normal amylose content, whereas  
77 another study using a different breeding strategy found increased amylose content to be  
78 accompanied with a loss of crystallinity (Hung et al., 2008).

79

80 The varieties used in this study, and those described by Blazek and Copeland (2008) and  
81 Hung et al. (2008), were obtained by genetic back-crossing of wheat cultivars grown in  
82 Australia. The swelling power test was used as a simple screening method to select lines for  
83 increased amylose content; hence, the genetic background of these wheat cultivars was not  
84 uniform. These starches have been shown to have a gradation of pasting, swelling and  
85 thermodynamic characteristics correlated to amylose content (Blazek & Copeland, 2008;  
86 Hung et al., 2008). In this study, SAXS together with DSC, XRD and fluorophore-assisted  
87 capillary electrophoresis, were employed to further examine structural features that provide  
88 these starches with a wide range of functional properties within a narrow range of enriched  
89 amylose content.

90

## 91 **MATERIALS AND METHODS**

92

### 93 *Materials*

94

95 Twelve wheat (*Triticum aestivum L.*) varieties selected from the set of samples described by  
96 Blazek & Copeland (2008) were used in the study. These included ten varieties with increased  
97 amylose content produced through the Value Added Wheat CRC Pty Ltd (VAWCRC)  
98 breeding program, one waxy variety and starch extracted from commercial flour. This  
99 breeding program is based on commercial Australian hard wheat cultivars of diverse genetic

100 background. Samples used in the study were grown in Eastern Australia over three growing  
101 seasons. Starch was extracted from flour using a two-step procedure that involved enzymic  
102 removal of proteins and subsequent extraction of free lipids with ethanol, based on the method  
103 of Akerberg et al. (1998) as described by Blazek & Copeland (2008).

104

105 Total amylose (T-AM) and free amylose (F-AM) content were determined by iodine binding  
106 as described by Chrastil (1987) using a calibration curve derived from a set of maize starches  
107 with zero to 75% amylose. According to this method, total and free amylose values were  
108 obtained from iodine binding with and without lipid extraction by ethanol, respectively.

109 Lipid-complexed amylose (L-AM) was calculated as the difference between T-AM and F-  
110 AM. Amylopectin chain length distribution was determined in the laboratories of CSIRO  
111 Plant Industry, Canberra, by fluorophore-assisted capillary electrophoresis using the Beckman  
112 P/ACE System 5010, as described by Morell et al. (1998) and O'Shea et al. (1998).

113

114 Starch swelling power (SSP) was determined by measuring water uptake at 92.5°C by a 40  
115 mg sample of starch according to the method of Konik-Rose et al. (2001) as described by  
116 Blazek & Copeland (2008). The swelling power test was carried out in 0.1% AgNO<sub>3</sub> solution  
117 to inhibit  $\alpha$ -amylase activity. Particle size distribution was determined in the laboratories of  
118 Allied Mills, Sydney using a Mastersizer laser diffraction instrument in wet-cell mode. Prior  
119 to analysis, starch samples were dispersed in deionized water and filtered through a 63  $\mu$ m  
120 sieve. Results are presented as the ratio of particles of diameter less than 10  $\mu$ m (assumed to  
121 be mostly B granules) to particles with diameter between 10 and 35  $\mu$ m (assumed to be  
122 mostly A granules).

123

124 *Small angle X-ray scattering*

125

126 SAXS measurements were obtained with a Bruker Nanostar SAXS camera, with pin-hole  
127 collimation for point focus geometry. The X-ray source was a copper rotating anode (0.1 mm  
128 filament) operating at 50 kV and 24 mA, fitted with cross coupled Göbel mirrors, resulting in  
129 a Cu  $K_{\alpha}$  radiation wavelength of 1.5418 Å. The SAXS camera was fitted with a Hi-star 2D  
130 detector (effective pixel size 100  $\mu\text{m}$ ). The sample to detector distance was chosen to be 650  
131 mm, which provided a  $q$ -range from 0.02 to 0.3 Å<sup>-1</sup>, where  $q$  is the magnitude of the scattering  
132 vector defined as:

$$133 \quad q = \frac{4\pi}{\lambda} \sin \theta,$$

134 with  $\lambda$  the wavelength and  $2\theta$  the scattering angle. Starch samples were presented in 2 mm  
135 sealed glass capillaries. Scattering data of starch samples were collected as starch suspensions  
136 containing excess water above the settled starch granules. SAXS curves of waxy starch and  
137 starch extracted from commercial flour were collected once only, whereas 9 replicate SAXS  
138 curves of the 10 starch samples from the VAWCRC were collected using separate capillaries;  
139 the enhanced precision offered by measuring sufficient replicates allowed subtle differences  
140 in lamellar architecture to be discerned. The optics and sample chamber were under vacuum  
141 to minimize air scattering. Scattering files were normalized to sample transmission, and after  
142 subtracting background, averaged radially using macros written in the Igor software  
143 (Wavemetrics, Lake Oswego, Oregon, USA). SAXS curves were plotted as a function of  
144 relative peak intensity,  $I$ , versus  $q$ , the scattering vector.

145

146 The parameters of the SAXS peaks of the varieties with increased amylose content, namely  
147 the thickness of the lamella and thicknesses of the crystalline and amorphous regions of the  
148 lamella, were determined by considering the ideal lamellar model, which consists of  
149 alternating crystalline and amorphous lamellae that are placed in stacks with dimensions that

150 are large enough not to affect the small angle scattering (Balta Calleja & Vonk, 1989;  
151 Koberstein & Stein, 1983; Strobl & Schneider, 1980). The model is assumed to be isotropic,  
152 that is it has no preferred orientation. Extrapolated scattering curves were Fourier transformed  
153 into a one dimensional correlation function using the CORFUNC program (part of the CCP13  
154 suite of software). The correlation function was interpreted in terms of an ideal lamellar  
155 morphology using Igor software and a curve fitting approach to obtain structural parameters  
156 describing the sample, namely the long period  $L_p$  (also known as Bragg spacing  $d$  or lamellar  
157 repeat distance), hard block thickness  $L_c$  and soft block thickness  $L_a$ . Electron density contrast  
158 was calculated from the one dimensional correlation function. The intensity of the scattering  
159 peak was determined by the graphical method as described by Yuryev et al. (2004). Waxy and  
160 commercial samples used in this study were analyzed by the same graphical method to  
161 determine repeat distance and peak intensity.

162

163 An alternative approach is to invoke the model proposed by Daniels and Donald (2003).  
164 However, this model utilizes eight adjustable parameters to account for the small-angle  
165 scattering. In the absence of additional scattering information, such as that obtained with  
166 combined neutron contrast variation methods and subsequent simultaneous global refinement,  
167 this method produces significant uncertainties in the fitting parameters, which limits its  
168 application. Hence, we used the simpler approach to allow comparison to be made between  
169 samples.

170

171 *X-ray diffraction*

172

173 XRD measurements of starch samples were made with a Difftech Mini Materials Analyser X-  
174 ray diffractometer (GBC Scientific Equipment Pty. Ltd.). The X-ray generator was equipped

175 with a cobalt anode ( $\lambda = 1.78897 \text{ \AA}$ ) operating at 1 kW and 3.36 mA. X-ray diffractograms  
176 were acquired at room temperature ( $20 \pm 1^\circ\text{C}$ ) over the  $2\theta$  range of  $5^\circ$  to  $35^\circ$  at a rate of  $0.50^\circ$   
177  $2\theta$  per minute and a step size of  $0.05^\circ 2\theta$ . Traces software v. 6.7.13 (GBC Scientific  
178 Equipment Pty. Ltd.) was used to manually subtract the background representing the  
179 amorphous portion of diffractograms. Starch crystallinity was calculated as a ratio of the  
180 crystalline area to the amorphous area. Perfection of the crystalline structures of the samples  
181 was assessed based on the full width at half maximum values of selected peaks typical for  
182 type A crystallinity.

183

#### 184 *Differential scanning calorimetry*

185

186 DSC measurements were made using a Modulated Differential Scanning Calorimeter MDSC  
187 2920 instrument (TA Instruments Inc., Delaware, USA). Starch and deionized water were  
188 weighed directly into an aluminum pan at a starch:water ratio of 1:2, and the pan was  
189 hermetically sealed. An empty pan was used as a reference. The pans were heated from 30 to  
190  $140^\circ\text{C}$  with the temperature increased at a rate of  $10^\circ\text{C}/\text{min}$ . The instrument was calibrated  
191 using indium as a standard. Melting temperatures were determined from the thermograms by  
192 means of the Universal Analysis 2000 software provided by the instrument company.  
193 Calorimetric enthalpy ( $\Delta H_m$ ) was determined by numerical integration of the area under the  
194 peak of thermal transition above the extrapolation lines. The average values of the  
195 thermodynamic parameters were determined using duplicate measurements and normalized  
196 per mole of anhydroglucose units ( $162 \text{ g mol}^{-1}$ ).

197

#### 198 *Scanning electron microscopy*

199

200 Electron micrographs of the starch granules were acquired with a Philips XL30 scanning  
201 electron microscope. Samples were mounted on double-sided carbon tape, coated with gold  
202 and imaged under an accelerating voltage of 10 kV.

203

204 *Statistical analysis*

205

206 All chemical analyses were performed using separate duplicate samples. Correlation analysis  
207 was performed using XLStat software (Addinsoft, New York, NY). Pearson's correlation  
208 coefficients ( $r$ ) were calculated between pairs of measured characteristics. A statistically  
209 significant relationship between two variables is indicated at the level of statistical  
210 significance of  $p < 0.05$ . The minimum  $r$  value for significance at  $p = 0.05$  for  $n = 10$  samples  
211 is 0.632. The starch from the waxy wheat and commercial flour were excluded from the  
212 statistical analysis so as not to distort the correlation coefficients by artificially increasing the  
213 range of measured characteristics. Moreover, the samples from the VAWCRC program were  
214 grown, stored and milled under similar conditions, whereas the waxy line and commercial  
215 sample were provided as flours.

216

## 217 **RESULTS**

218

219 *Composition and pasting properties of wheat starches*

220

221 The composition, swelling properties, melting temperature and chain length distribution of  
222 amylopectin of the starches isolated from the cultivars used in this study are summarized in  
223 Table 1. Excluding the starches from the waxy wheat and commercial flour, these starches  
224 had between 53 and 59% of particles with size distribution between 10 and 35  $\mu\text{m}$  (assumed

225 to be mainly A granules). Total, free and lipid-complexed amylose content varied between 36  
226 and 43%, 28 and 33% and 6 and 14%, respectively. Starch swelling power ranged between  
227 5.4 and 6.9 (Table 1).

228

229 Starch extracted from the commercial flour had 35% total amylose, swelling power of 6.3 and  
230 contained 57% of particles with size distribution between 10 and 35  $\mu\text{m}$ . The waxy wheat  
231 variety included in the study as a comparison, had 4% total amylose content and contained  
232 48% of supposed A granules. Swelling power of the isolated waxy starch was not measurable  
233 by the method used in this study.

234

235 Scanning electron micrographs of starch granules of the waxy variety and of the amylose-rich  
236 varieties (SM1118 is shown as a representative) indicated there were no obvious  
237 morphological differences between the granules of the starches examined in this study (Fig.  
238 1). Granules smaller than 10  $\mu\text{m}$  in diameter - assumed to be B granules - displayed round,  
239 ellipsoidal, as well as angular and irregular shapes. The surface of most of the granules with  
240 diameter greater than 10  $\mu\text{m}$  from all studied wheat varieties displayed indentations, which  
241 are likely to be caused by impressions from B granules and protein bodies.

242

243 *Amylopectin chain length distribution*

244

245 The amylopectin chains were classified into four fractions according to chain length. These  
246 were short chains with degree of polymerization (DP) 6 to 12, medium length chains with DP  
247 13 to 24, long chains with DP 25 to 36, and very long chains with DP greater than 36. The  
248 proportions of the fractions in all of the samples were 41 to 45% of short chains, 46 to 49% of  
249 medium length chains, 7 to 9% of long chains and less than 2% of very long chains (Table 1).

250 Starches from VAWCRC breeding program had smaller proportions of short chains and  
251 greater proportions of long chains as compared to the waxy and commercial starches. No  
252 apparent trends or differences were observed among the starches from VAWCRC breeding  
253 program (Table 1).

254

255 *Crystallinity and thermal characteristics*

256

257 XRD patterns of the selected starches are shown in Fig. 2. All of the starches studied  
258 displayed A-type crystallinity with peaks at 17.6, 19.9, 20.8 and 26.7° 2 $\theta$ . Based on the full  
259 width at half maximum of the characteristic peaks, waxy wheat displayed the most perfect  
260 crystalline structures, whereas the commercial starch showed the least perfect crystallites. The  
261 XRD patterns of the 10 varieties from the VAWCRC program were qualitatively very similar  
262 and differences in total crystallinity and perfection of the crystal structures could not be  
263 quantified due to inherent uncertainties of the method related to the definition of the  
264 amorphous background and peak overlay. A peak fitting procedure described by Lopez-Rubio  
265 et al. (2008) may allow calculation of starch crystallinity and contribution from the different  
266 crystal polymorphs of starch to the total crystallinity, but the quality of the experimental data  
267 and differences among traces were not sufficient to use this method.

268

269 DSC data showed that the gelatinization temperatures of starches isolated from the varieties  
270 from the VAWCRC program varied from 61.5 to 65.4°C (Table 1). Waxy wheat had higher  
271 melting temperature of 66.8°C, consistent with the increased degree of crystallinity observed  
272 by XRD. Starch from the commercial flour had a melting temperature of 62.1°C. Based on the  
273 area under the peak of thermal transition, the transition enthalpy of waxy starch was 1,303

274 kJ/mol, whereas the enthalpies of the commercial starch and variety SM1046 were 996 kJ/mol  
275 and 1,211 kJ/mol, respectively (Fig. 3).

276

277 *SAXS characteristics*

278

279 The SAXS patterns from several of the starches used in this study are shown in Fig. 4. The  
280 values of the parameters obtained from the scattering profile as described in the Methods  
281 section varied significantly among the varieties, as shown in Table 1. Long period,  $L_p$ , ranged  
282 between 91.8 and 94.7 Å for the starches from the VAWCRC program. The thickness of the  
283 crystalline region of the lamella (hard block),  $L_c$ , and amorphous region (soft block) thickness,  
284  $L_a$ , varied from 68.4 to 70.9 Å and from 23.4 to 23.9 Å, respectively (Table 1). Fig. 5 shows  
285 nine replicate values of  $L_p$  for each of the 10 samples. The variation among the replicates of  
286 each sample was within approximately 1 Å (Fig. 5). The variation in the intensity of the  
287 scattering peak within the 9 replicates was comparable in magnitude to the variation among  
288 individual samples (data not shown). A similar observation was made for electron density  
289 contrast values calculated from the one dimensional correlation function. Therefore, these two  
290 parameters were not used in the statistical correlation analysis.

291

292 As determined by the graphical method of Yuryev et al. (2004), the waxy starch and  
293 commercial variety had repeat distances of 99.6 Å and 108.3 Å, respectively. As a  
294 comparison, graphical analysis performed on one of the replicate SAXS curves of variety  
295 SM1046 yielded a repeat distance of 110.2 Å. It is worth noting that the average repeat  
296 distance as determined by the correlation function analysis (Table 1) is about 15% smaller  
297 than the Bragg distance  $d$ , and this is in agreement with results reported by others (Jenkins et  
298 al., 1993; Yuryev et al., 2004).

299

300 Correlations of the parameters obtained from the SAXS peak with selected chemical and  
301 functional characteristics of the starch varieties used in this study (excluding the waxy wheat  
302 and starch from commercial starch) are summarized in Table 2. Positive correlation  
303 (significant at  $p < 0.05$ ) was found between  $L_p$  and T-AM ( $r = 0.75$ , Fig. 6). Similarly,  
304 correlations were found between hard and soft block thicknesses and T-AM, with correlation  
305 coefficients of 0.749 and 0.669, respectively. Melting temperature and amylopectin chain  
306 length distribution did not correlate significantly with any of the studied characteristics.

307

## 308 **DISCUSSION**

309

### 310 *Repeatability of SAXS measurement*

311

312 As shown by the spread of nine replicate values of  $L_p$  for each of the 10 samples studied (Fig.  
313 5), the repeatability of individual measurements was within a range of approximately 1 Å. In  
314 comparison, the variation of  $L_p$  among the samples with amylose content between 35 and 43%  
315 was of the order of 3 Å. Uncertainty may exist as to whether the magnitude of the  
316 experimental error allows meaningful differentiation of such samples, given their amylose  
317 content falls within a narrow range. However, our study illustrates that SAXS may provide  
318 information regarding the lamellar architecture in sample sets that differ in  $L_p$  by only a few  
319 angstroms and that a significant correlation exists between the lamellar repeat and amylose  
320 content.

321

322

323 The scattering intensity for a simple two phase system is proportional to the product of the  
324 relative fractions of each phase and the scattering length density difference (Glatter & Kratky,  
325 1982; Higgins & Benoit 1997). In agreement with this scattering theory and according to  
326 Yuryev et al. (2004), the intensity of the scattering peak ( $I_{max}$ ) depends on the amount of the  
327 ordered semi-crystalline structures and/or on the differences in electron density between  
328 crystalline and amorphous layers. Because the degree of crystallinity in the starches studied  
329 did not vary significantly as shown by the XRD, we propose that the observed changes in  $I_{max}$   
330 mainly reflect the difference in the electron density between the crystalline and amorphous  
331 regions of the lamellar structure. The fact that the variation in  $I_{max}$  values among replicate  
332 measurements was comparable in magnitude to the variation between samples may be  
333 attributed to variations in packing density of individual capillaries influencing the scattering  
334 intensity to an extent that exceeds any correlation. As a result, natural variation between  
335 sample preparations may outweigh any real correlations. The development of a more  
336 reproducible method to avoid such variations in the packing density of these starch slurries  
337 would help overcome this issue.

338

339 *Effect of amylose content on the structural parameters of starch granules*

340

341 The results of several studies have shown that lamellar repeat distance of starches from  
342 different botanical sources varies within a range between 9 and 11 nm, and that XRD patterns  
343 show little variability within plant species (Kozlov et al., 2007a; Vandeputte & Delcour,  
344 2004; Yuryev et al., 2004). However, starch granules extracted from different plant sources  
345 are usually considered to display decreasing intensity of the scattering maximum with  
346 increasing amylose content (Bocharnikova et al., 2003; Jenkins & Donald, 1995; Kozlov et  
347 al., 2007a, 2007b; Sanderson et al., 2006; Yuryev et al., 2004). This trend is accounted for by

348 a decrease in the difference in electron density between the crystalline and amorphous regions  
349 of the lamellae with increasing amylose content. Kozlov et al. (2007b) suggested that an  
350 increase in amylose content is accompanied both by accumulation of amylose tie-chains in  
351 amylopectin clusters forming defects in crystalline lamellae, and by disordered amylose  
352 chains within amorphous regions. Disordered ends of amylopectin double helices and/or  
353 double helices not participating in the formation of crystals are also proposed to be  
354 contributing factors to defects of the crystalline regions and, in turn, to greater disorder in the  
355 packing of the lamellar structure (Koroteeva et al., 2007a, b; Kozlov et al., 2007b). The  
356 occurrence of amylose-amylose double helices within the crystalline lamellar regions  
357 containing mainly amylopectin double helices has been shown to be highly unlikely in native  
358 starch granules and is not considered as a possible explanation for the intensity decrease  
359 (Kalichevsky & Ring, 1987; Tester et al., 2000).

360

361 Positive correlations between  $L_p$  and amylose content, and between hard and soft block  
362 thicknesses and amylose content, indicate that amylose accumulates in both crystalline and  
363 amorphous parts of the lamellae (Table 2 & Fig. 6). This hypothesis is consistent with current  
364 understanding of starch synthesis, which considers that amylose and amylopectin are  
365 synthesized simultaneously (reviewed by Morell et al., 2003). If thickness of one of the  
366 lamellar regions remained constant as the amylose content varies, it would be more difficult to  
367 explain how amylose and amylopectin are synthesized together and packed into the granule.

368

369 It has been reported that an increase in amylose content would be expected to be accompanied  
370 by decreasing crystallinity, decreasing melting enthalpy and decreasing values of melting  
371 temperature of the amylopectin crystallites in native wheat starch granules with amylose  
372 content less than 50% (Koroteeva et al., 2007a, b; Kozlov et al., 2007b). In agreement with

373 results by Hung et al. (2008), our results did not confirm these trends. Insignificant  
374 differences in total crystallinity and the lack of correlation between  $T_m$  and any of the studied  
375 characteristics within the set of varieties from VAWCRC program indicates that there may be  
376 several underlying factors affecting lamellar structure that may mask general trends that occur  
377 over a wider range of amylose content. Increased defects in the crystalline lamella with  
378 increasing amylose content may to some extent be compensated by a protective effect of  
379 amylose in the amorphous lamellar regions on the crystallites, consistent with increased soft  
380 block thickness being correlated with increasing amylose content.

381

382 The SAXS curves shown in Fig. 4 indicate that the contrast in electron density between hard  
383 and soft blocks of waxy starch is significantly greater than in the other starches, even when  
384 underlying variability in scattering peak intensity is considered. When the waxy wheat variety  
385 was compared with the other varieties used in this study, the following trends were observed:  
386 the waxy variety had more sharply defined XRD peaks, smaller repeat distance, higher  
387 intensity of the SAXS peak, higher melting temperature, and higher melting enthalpy. Based  
388 on combined results acquired by SAXS, DSC and XRD analyses, we conclude that the  
389 differences between the waxy variety and the other samples used in this study are due to  
390 amylose defects accumulating in the crystalline regions as well as more amylose  
391 accumulating in the amorphous regions of lamellar structure. The higher melting temperature,  
392 more sharply defined XRD peaks and greater intensity of SAXS peak observed for the waxy  
393 starch are consistent with the hypothesis that amylopectin crystallites have fewer defects in  
394 waxy starch than in amylose-rich starches. The larger lamellar repeat distance observed for  
395 the non-waxy starches provides evidence for more amylose accumulating in both crystalline  
396 and amorphous regions of the lamellae in amylose-rich starches.

397

398 Starch extracted from commercial flour had amylose content between that of waxy wheat and  
399 the set of wheat varieties from VAWCRC. Accordingly, intensity of the scattering peak and  
400 repeat distance of the commercial starch was between that of waxy wheat and the VAWCRC  
401 varieties. However, perfection of XRD peaks, melting temperature and transition enthalpy  
402 were lower than in starches from the VAWCRC varieties. We propose that crystallinity and  
403 thermal characteristics, but not electron density contrast and lamellar thicknesses, of the  
404 commercial starch may have been affected by commercial milling, for example by inclusion  
405 of a grain tempering step.

406

407 Lamellar spacing, as indicated by  $L_p$ , did not increase continuously with increasing amylose  
408 content, but rather the 10 samples segregated into two groups, with a step increase in  $L_p$   
409 between them (Fig. 6). The two groups were not differentiated by growing season, and hence  
410 this distribution is likely to reflect underlying genetic variation and/or environmental  
411 influences on the expression and activities of enzymes involved in starch synthesis.

412

413 Over a wide range of amylose content, three main factors are considered to influence the  
414 structural parameters of native starch granules at the nanoscale: (i) amylose defects located in  
415 the crystalline region of the lamellae (both as amylose tie-chains and amylose-lipid  
416 complexes), (ii) the amount of amylose within the amorphous regions of the lamellae, and (iii)  
417 chain length distribution of amylopectin chains (Koroteeva et al., 2007a, b; Kozlov et al.,  
418 2007b). When structural characteristics of the group of amylose-rich starches used in this  
419 study were compared with waxy wheat starch, the general trend described by Kozlov et al.  
420 (2007b) was confirmed. However, our results indicate that increasing amylose content within  
421 a narrow range of elevated amylose content is not necessarily accompanied by increased  
422 accumulation of crystal defects. In general, the structure of wheat starches from different

423 varieties, and their functional properties, appear to be determined by amylose content, but fine  
424 structural variations brought about by differences in genetic background introduces  
425 uncertainty into the prediction of functional properties from amylose content alone.

426

427

## 428 **CONCLUSIONS**

429

430 Analysis of starches with amylose content between 35 and 43% showed SAXS may provide  
431 information regarding the lamellar architecture in sample sets that differ in  $L_p$  by only a few  
432 angstroms and that a significant correlation exists between the lamellar repeat and amylose  
433 content. The results of the SAXS analysis of the wheat starches were consistent with amylose  
434 accumulating in both crystalline and amorphous parts of the lamellae. We conclude that  
435 amylose content directly affects the organization of semicrystalline lamellae within granules,  
436 whereas thermodynamic properties are influenced more by the interplay between amylose  
437 content and amylopectin architecture.

438

439

## 440 **ACKNOWLEDGEMENTS**

441

442 J. B. was supported by a scholarship from the Value Added Wheat CRC Pty Ltd. The authors  
443 acknowledge the facilities as well as scientific and technical assistance from staff in the  
444 NANO Major National Research Facility at the Electron Microscope Unit, The University of  
445 Sydney. The authors are grateful to Allied Mills for use of the laboratory mill Quadramat  
446 Junior and Mastersizer particle size instrument. The authors are also grateful to CSIRO Plant

447 Industries, Canberra for making available the Beckman P/ACE System 5010 Capillary  
448 Electrophoresis Instrument and to Oscar Larroque for assistance with the analysis.

449

450

## 451 REFERENCES

452

453 Akerberg, A. K. E., Liljeberg, H. G. M., Granfeldt, Y. E., Drews, A. W., & Bjorck, I. M. E.  
454 (1998). An in vitro method, based on chewing, to predict resistant starch content in foods  
455 allows parallel determination of potentially available starch and dietary fiber. *Journal of*  
456 *Nutrition*, 128, 651-660.

457

458 Balta Calleja, F. J., & Vonk, C. G. X-ray Scattering of Synthetic Polymers, Elsevier,  
459 Amsterdam, 1989, 247-257.

460

461 Blanshard, J. M. V., Bates, D. R., Muhr, A. H., Worcester, D. L., & Higgins, J. S. (1984).  
462 Small angle neutron scattering studies of starch granule structure. *Carbohydrate Polymers*, 4,  
463 427-442.

464

465 Blazek J., & Copeland L. (2008). Pasting and swelling properties of wheat flour and starch in  
466 relation to amylose content. *Carbohydrate Polymers*, 71, 380-387.

467

468 Bocharnikova, I., Wasserman, L. A., Krivandin, A. V., Fornal, J., Baszczak, W., Chernykh,  
469 V. Y., Schiraldi, A., & Yuryev, V. P. (2003). Structure and thermodynamic melting  
470 parameters of wheat starches with different amylose content. *Journal of Thermal Analysis and*  
471 *Calorimetry*, 74, 681-695.

472

473 Cameron, R. E., & Donald, A. M. (1992). A small-angle X-ray scattering of study of the  
474 annealing and gelatinisation of starch. *Polymer*, 33, 2628-2635.

475

476 Chrastil, J. (1987). Improved colourimetric determination of amylose in starches of flours.  
477 *Carbohydrate Research*, 159, 154-158.

478

479 Daniels, D. R., & Donald, A. M. (2003). An improved model for analyzing the small angle x-  
480 ray scattering of starch granules. *Biopolymers*, 69, 165-165.

481

482 Donald, A. M., Kato, K. L., Perry, P. A., & Waigh, T. A. (2001). Scattering studies of the  
483 internal structure of starch granules. *Starch/Stärke*, 53, 504-512.

484

485 Glatter, O., & Kratky, O. (1982). Small-angle X-ray scattering. Academic Press, New York.

486

487 Higgins, J. S., & Benoit, H. C. (1997). Polymers and Neutron Scattering. Oxford University  
488 Press, pp. 124.

489

490 Hung, P.V., Maeda, T., Miskelly, D., Tsumori, R., & Morita, N. (2008). Physicochemical  
491 characteristics and fine structure of high-amylose wheat starches isolated from Australian  
492 wheat cultivars. *Carbohydrate Polymers*, 71, 656-663.

493

494 Hung, P. V., Maeda, T., & Morita, N. (2007). Study on physicochemical characteristics of  
495 waxy and high-amylose wheat starches in comparison with normal wheat starch.  
496 *Starch/Stärke*, 59, 125-131.

497

498 Jenkins, P. J., Cameron, R. E., & Donald, A. M. (1993). A universal feature in the structure of  
499 starch granules from different botanical sources. *Starch/Stärke*, 45, 417-420.

500

501 Jenkins, P. J., & Donald, A. M. (1995). The influence of amylose on starch granule structure.  
502 *International Journal of Biological Macromolecules*, 17, 315-321.

503

504 Kalichevsky, M. T., & Ring, S. G. (1987). Incompatibility of amylose and amylopectin in  
505 aqueous solution. *Carbohydrate Research*, 162, 323-328.

506

507 Koberstein, J. T., & Stein, R. J. (1983). Small-angle x-ray scattering measurements of diffuse  
508 phase-boundary thicknesses in segmented polyurethane elastomers. *Journal of Polymer*  
509 *Science: Polymer Physics Edition*, 21, 2181-2200.

510

511 Koroteeva, D. A., Kiseleva, V. I., Krivandin, A. V., Shatalova, O. V., Błaszczak, W., Bertoft,  
512 E., Piyachomkwan, K., & Yuryev, V. P. (2007a). Structural and thermodynamic properties of  
513 rice starches with different genetic background. Part 2. Defectiveness of different  
514 supramolecular structures in starch granules. *International Journal of Biological*  
515 *Macromolecules*, 41, 534-547.

516

517 Koroteeva, D. A., Kiseleva, V. I., Sriroth, K., Piyachomkwan, K., Bertoft, E., Yuryev, P. V.,  
518 & Yuryev, V. P. (2007b). Structural and thermodynamic properties of rice starches with  
519 different genetic background. Part 1. Differentiation of amylopectin and amylose defects.  
520 *International Journal of Biological Macromolecules*, 41, 391-403.

521

- 522 Konik-Rose, C. M., Moss, R., Rahman, S., Appels, R., Stoddard, F., & McMaster, G. (2001).  
523 Evaluation of the 40 mg swelling test for measuring starch functionality. *Starch/Stärke*, 53,  
524 14-20.
- 525
- 526 Kozlov, S. S., Blennow, A., Krivandin, A. V., & Yuryev, V. P. (2007a). Structural and  
527 thermodynamic properties of starches extracted from GBSS and GWD suppressed potato  
528 lines. *International Journal of Biological Macromolecules*, 40, 449-460.
- 529
- 530 Kozlov, S. S., Krivandin, A. V., Shatalova, O. V., Noda, T., Bertoft, E., Fornal, J., & Yuryev,  
531 V. P. (2007b). Structure of starches extracted from near-isogenic wheat lines. Part II.  
532 Molecular organization of amylopectin clusters. *Journal of Thermal Analysis and*  
533 *Calorimetry*, 87, 575–584
- 534
- 535 Kozlov, S. S., Noda, T., Bertoft, E., & Yuryev, V. P. (2006). Structure of starches extracted  
536 from near-isogenic wheat lines. Part I. Effect of different GBSS I combinations. *Journal of*  
537 *Thermal Analysis and Calorimetry*, 86, 291–301.
- 538
- 539 Lopez-Rubio, A., Htoon, A., & Gilbert, E. P. (2007). Influence of extrusion and digestion on  
540 the nanostructure of high-amylose maize starch. *Biomacromolecules*, 8, 1564-1572.
- 541
- 542 Lopez-Rubio, A., Flanagan, B. M., Gilbert, E.P. & Gidley, M. J. (2008). A novel approach for  
543 calculating starch crystallinity and its correlation with double helix content: a combined XRD  
544 and NMR study. *Biopolymers*, 89, 761-768
- 545

546 Matveev, Y. I., Elankin, N. I., Kalistratova, E. N., Danilenko, A. N., Niemann, C., & Yuryev,  
547 V. P. (1998). Estimation of contributions of hydration and glass transition to heat capacity  
548 changes during melting of native starches at excess water. *Starch/Stärke*, 50, 141–147.

549

550 Morell, M. K., Samuel, M. S., & O'Shea, M. G. (1998). Analysis of starch structure using  
551 fluorophore-assisted carbohydrate electrophoresis. *Electrophoresis*, 19, 2603-2611.

552

553 Morell, M. K., Regina, A., Li, Z., Hashemi, B. K., & Rahman, S. (2003). Advances in the  
554 understanding of starch synthesis in wheat and barley. *Journal of Applied Glycoscience*, 50,  
555 217-224.

556

557 Morell, M. K., & Myers, A. M. (2005). Towards the rational design of cereal starches.  
558 *Current Opinion in Plant Biology*, 8, 204–210.

559

560 O'Shea, M. G., Samuel, M. S., Konik, C. M., & Morell, M. K. (1998). Fluorophore-assisted  
561 carbohydrate electrophoresis (FACE) of oligosaccharides: efficiency of labelling and high-  
562 resolution separation. *Carbohydrate Research*, 307, 1-12.

563

564 Strobl, G. R., & Schneider, M. (1980). Direct evaluation of the electron density correlation  
565 function of partially crystalline polymers. *Journal of Polymer Science: Polymer Physics*  
566 *Edition*, 18, 1343-1359.

567

568 Tester, R. F., Debon, S. J. J., & Sommerville, M. D. (2000). Annealing of maize starch.  
569 *Carbohydrate Polymers*, 42, 287–299

570

- 571 Vandeputte, G.E., & Delcour, J.A. (2004). From sucrose to starch granule to starch physical  
572 behaviour: a focus on rice starch. *Carbohydrate Polymers*, 58, 245–266.  
573
- 574 Vermeulen, R., Derycke, V., Delcour, J. A., Goderis, B., Reynaers, H., & Koch, M. H. J.  
575 (2006). Gelatinization of starch in excess water: beyond the melting of lamellar crystallites. a  
576 combined wide- and small-angle X-ray scattering study. *Biomacromolecules*, 7, 2624–2630.  
577
- 578 Vermeulen, R., Goderis, B., Reynaers, H., Delcour J. A. (2005). Gelatinisation related  
579 structural aspects of small and large wheat starch granules. *Carbohydrate Polymers*, 62, 170-  
580 181.  
581
- 582 Waigh, T. A., Jenkins, P. J., & Donald, A. M. (1996). Quantification of water in carbohydrate  
583 lamellae using SANS. *Farraday Discussions*, 103, 325-337.  
584
- 585 Waigh, T. A., Gidley, M. J., Komanshek, B. U., & Donald, A. M. (2000a). The phase  
586 transformations in starch during gelatinisation: a liquid crystalline approach. *Carbohydrate*  
587 *Research*, 328, 165-176.  
588
- 589 Waigh, T. A., Kato, K. L., Donald, A. M., Gidley, M. J., & Riekkel. C. (2000b). Side-chain  
590 liquid crystalline model for starch. *Starch/Stärke*, 52, 252-260.  
591
- 592 Yuryev, V. P., Krivandin, A. V., Kiseleva, V. I., Wasserman, L. A., Genkina, N. K., Fornal,  
593 J., Blaszcakb, W., & Schiraldi, A. (2004). Structural parameters of amylopectin clusters and  
594 semi-crystalline growth rings in wheat starches with different amylose content. *Carbohydrate*  
595 *Research*, 339, 2683–2691.

596 Table 1. Summary of the properties of the starches used in this study.

597 Total (T-AM), free (F-AM) and lipid-complexed (L-AM) amylose content, and swelling  
 598 power of starch (SSP) were determined as described in the text. The percentage of A granules  
 599 was calculated from the particle size distribution as particles with diameter between 10 and  
 600 35  $\mu\text{m}$ . Melting temperature,  $T_m$ , was determined by DSC. Amylopectin chain length  
 601 distribution was divided into four groups according to the DP, as described in the text. Long  
 602 period  $L_p$ , hard block thickness  $L_c$  and soft block thickness  $L_a$  calculated from SAXS curves  
 603 as described in the text.

604

	T-AM (%)	F-AM (%)	L-AM (%)	SSP (ww)	A- granules (%)	$T_m$ (°C)	DP 6-12 (%)	DP 13-24 (%)	DP 25-36 (%)	DP>36 (%)	$L_p$ (Å)	$L_a$ (Å)	$L_c$ (Å)
Waxy starch	4.1	-	-	-	48.1	66.8	43.6	46.9	7.9	1.6	-	-	-
Commercial starch	35.2	29.5	5.7	6.3	57.3	62.1	45.0	46.2	7.4	1.4	-	-	-
Diamondbird	36.1	29.9	6.2	6.3	58.2	61.5	43.0	47.0	8.4	1.6	93.38	23.53	69.84
Ega Hume	36.8	30.7	6.2	6.9	58.0	65.0	41.9	47.7	8.7	1.8	92.91	23.54	69.37
Batavia	37.1	29.8	7.2	6.5	55.9	63.8	41.5	48.4	8.3	1.8	91.82	23.37	68.44
Pelsart	37.8	31.9	5.9	6.0	53.2	64.0	42.0	48.0	8.4	1.7	92.64	23.39	69.25
SM1 118	38.8	33.2	5.6	5.4	57.1	64.5	41.7	48.6	8.1	1.6	92.94	23.59	69.35
Minto	39.2	30.1	9.1	6.4	55.5	65.4	41.5	48.4	8.4	1.7	92.53	23.52	69.01
OA24-328-1	40.2	31.0	9.2	6.0	57.5	64.0	42.3	47.7	8.4	1.6	94.31	23.85	70.46
OA24-328-3	41.2	33.1	8.1	5.8	59.2	64.1	41.8	47.7	8.7	1.8	94.22	23.77	70.45
OA24-198-3	42.0	33.4	8.7	5.6	55.9	63.6	41.2	47.9	9.0	1.9	94.73	23.78	70.95
SM1046	42.8	28.6	14.2	6.1	58.6	65.0	43.2	47.3	7.9	1.6	94.13	23.60	70.53

605

606

607

608

609

610

611

612 Table 2. Correlation matrix between physicochemical and structural characteristics, based on  
 613 the 10 samples used in this study. Values in bold indicate significant correlations at a  
 614 significance level  $\alpha=0.05$ , minimum  $r$  to be significant at  $p=0.05$  for  $n = 10$  samples is  
 615 0.632. Total (T-AM), free (F-AM) and lipid-complexed (L-AM) amylose content, and  
 616 swelling power of starch (SSP) were determined as described in the text. The percentage of A  
 617 granules was calculated from the particle size distribution as particles with diameter between  
 618 10 and 35  $\mu\text{m}$ . Melting temperature,  $T_m$ , was determined by DSC. Amylopectin chain length  
 619 distribution was divided into four groups according to the DP, as described in the text. Long  
 620 period  $L_p$ , hard block thickness  $L_c$  and soft block thickness  $L_a$  calculated from SAXS curves  
 621 as described in the text.

622

623

	T-AM	F-AM	L-AM	SSP	A-granules	Tm	DP 6-12	DP 13-24	DP 25-36	DP>36
Lp	<b>0.752</b>	0.299	0.483	-0.481	0.482	-0.135	0.239	-0.538	0.336	0.049
La	<b>0.669</b>	0.421	0.330	-0.467	0.512	-0.016	-0.017	-0.254	0.391	0.148
Lc	<b>0.749</b>	0.267	0.501	-0.472	0.463	-0.156	0.285	-0.581	0.316	0.028
Tm	0.368	-0.044	0.360	0.113	-0.070	1	-0.291	0.475	-0.189	0.141

624

625

626 **Figure captions**

627

628 Figure 1. SEM micrographs of waxy wheat starch granules (a) and SM1118 starch granules  
629 (b).

630 Figure 2. X-ray diffraction patterns of wheat varieties used in this study. Waxy wheat (a),  
631 commercial starch (b) and. SM1046 (c).. The traces have been offset for clarity of  
632 presentation.

633

634 Figure 3. DSC gelatinization characteristics of selected wheat varieties used in this study.  
635 Heat flow was measured in cal/sec/g and the traces have been offset for clarity of  
636 presentation. Starch to water ratio 1:2, heated at 10°C/min.

637

638 Figure 4. SAXS patterns of several of the starch varieties used in this study. The traces were  
639 obtained as described in the Methods section.

640

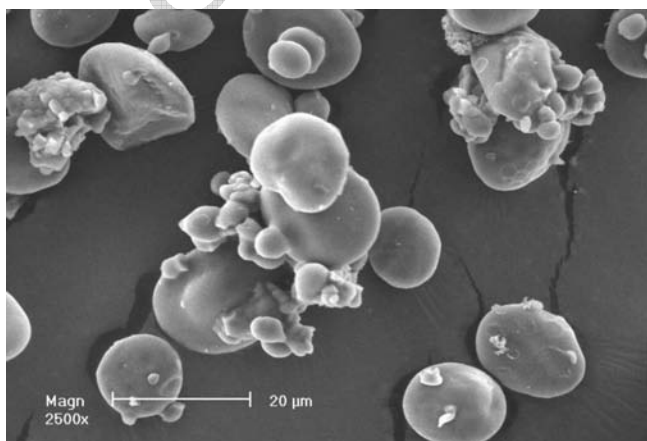
641 Figure 5. Variability in long period based on nine replicates shown for 10 samples used in this  
642 study.

643

644 Figure 6. Amylose content vs. long period. Error bars show standard deviations based on nine  
645 replicates.

646

ACCEPTED MANUSCRIPT



ACCEPTED MANUSCRIPT

